

NASA TECHNICAL TRANSLATION

~~N 70 39839~~  
N 70 39939  
NASA TT F-13,260

QUASI-TWO-DIMENSIONAL FLOW THROUGH A SUPERSONIC CASCADE

J. Jehl

CASE FILE  
COPY

Translation of "Écoulement Supersonique Quasi-Bidimensionnel dans une Grille D'aubes Supersonique". La Recherche Aéronautique, No. 3, May-June 1970, pp. 137 - 143.

NATIONAL AERONAUTICS AND SPACE ADMINISTRATION  
WASHINGTON D. C., 20546 SEPTEMBER 1970

## QUASI TWO-DIMENSIONAL FLOW THROUGH A SUPERSONIC CASCADE

Joseph Jehl<sup>(1)</sup>

ABSTRACT. A theoretical scheme in which the influence of the transverse stream contraction in a compressor or turbine cascade on the supersonic flow crossing this cascade is taken into account. The numerical method developed in this theoretical scheme may also be adapted to the case of a flow variation in the stream.

### I. Introduction

/137\*

The strong compression ratios in supersonic compressors lead to the adaptation of non-cylindrical external contours of these machines. The analysis of the flow in these blade grills, which is performed by making a cylindrical cut of the rotor and developing it onto a plane, must take into account the radial component of velocity. The importance of this term increases as the stream convergence increases and also increases with the radial gradient of the enthalpy. The classical two-dimensional method of studying supersonic flows in blade grills ceases to have validity. However, the three-dimensional calculation of the flow in all its generality would make it necessary to use methods which would be too difficult to be of any practical use. This is why we are presenting here an approximate quasi-two-dimensional method which is analogous to those studied by Shaalon and Horlock [1] and by Mani and Acosta [2] for the case of subsonic blade grills where the effects of the lateral stream contraction, variation of the axial velocity components and variations of the total yield are represented by a flow-model having a constant cross section.

/138

---

\* Numbers in the margin indicate the pagination in the original foreign text.

(1) Engineer at Société Brown Boveri, Baden (Switzerland).

The calculation presented here was programmed on an IBM 360-50 computer.

## II. Definition of the Problem

### II.1. Three-dimensional Flow in a Supersonic Blade Grill

The three-dimensional effect in a blade grill can be due to the following:

a) In a smooth wind-tunnel with supersonic blade grills the progressive thickening of the boundary layers along the lateral side of the tunnel reduces the cross section available for passage of the undisturbed flow. In a flow having a cross section, this effect can be represented by parietal injection of fluids;

b) In a cross section of a compressor, a radial displacement of the stream surfaces brings about a radial gradient of the yield. An average value of this gradient can be obtained by means of the condition of conservation of the global yield of the machine and a condition of radial equilibrium of the stream at the output of the grill.

We will only study the first case here, but the generalization of the calculations to the study of a compressor cross section will not encounter with any difficulty.

### II.2. Quasi-Two-Dimensional Flow in a Supersonic Cascade.

Let us consider the motion of a perfect fluid in a constant cross section. Due to the fact that the lateral walls are parallel, equations of motion are written:

$$\begin{cases} \frac{\partial p}{\partial x} + \rho u \frac{\partial u}{\partial x} + \rho v \frac{\partial u}{\partial y} = 0 \\ \frac{\partial p}{\partial y} + \rho u \frac{\partial v}{\partial x} + \rho v \frac{\partial v}{\partial y} = 0 \end{cases} \quad (1)$$

where  $(u, v)$  are average values of the velocity components, normal and parallel to the front of the cascade, respectively, taken at the transverse height  $h$  of the channel.  $P$  and  $\rho$  are the average corresponding pressure and volume mass density, respectively, and the coordinate system  $(x, y)$  is defined in such a way that the  $Oy$  axis coincides with the front of the cascade and the  $Ox$  axis is parallel to the incoming velocity (Figure 1).

The equation of mass conservation is written as:

$$\frac{\partial(\rho u)}{\partial x} + \frac{\partial(\rho v)}{\partial y} + \frac{\rho w_p}{h} = 0 \quad (2)$$

where  $W_p$  is the transverse velocity component of the velocity defined along the wall.

Since the flow is isoenergetic and the fluid is a perfect one, the flow is irrotational and  $a$  is the local sound velocity ( $a_0$  is the corresponding velocity at rest). The components  $(u, v)$  of the velocity are related by the relationships:

$$\begin{aligned} (a^2 - u^2) \frac{\partial u}{\partial x} - 2uv \frac{\partial u}{\partial y} + (a^2 - v^2) \frac{\partial v}{\partial y} - a^2 \frac{w_p}{h} &= 0 \\ \frac{\partial u}{\partial y} &= \frac{\partial v}{\partial x} \\ a^2 &= a_0^2 - \frac{\gamma - 1}{2} (u^2 + v^2) \end{aligned} \quad (3)$$

This generalizes the classical equations of two-dimensional motion of a compressible fluid through the case of a flow with parietal injection of fluid.

### II.3. Equations for the Characteristics of the Quasi-Two-Dimensional Motion

When the flow under consideration is supersonic (isoentropic flow is assumed with no shock waves and quasi-isoentropic flows is assumed when the shock waves

form in the interior of the fluids), two characteristics pass through each point of the physical plane (x, y). One characteristic is an ascending characteristic (I) and the other is a descending characteristic (II). The corresponding characteristics in the hodograph plane are related to them and are satisfied in equations: /139

$$\begin{aligned}
 & \frac{dy}{dx} = \frac{M^2 \sin \theta \cos \theta - \sqrt{M^2 - 1}}{M^2 \cos^2 \theta - 1} \\
 \text{(I)} \quad & \left\{ \begin{aligned} \frac{dM}{dx} &= - \frac{(2 + (\gamma - 1)M^2)M}{2\sqrt{M^2 - 1}} \frac{d\theta}{dx} - \frac{M_p}{h} \frac{2 + (\gamma - 1)M^2}{2[(M^2 - 1) \cos \theta + \sqrt{M^2 - 1} \sin \theta]} \end{aligned} \right. \\
 & \frac{dy}{dx} = \frac{M^2 \sin \theta \cos \theta + \sqrt{M^2 - 1}}{M^2 \cos^2 \theta - 1} \\
 \text{(II)} \quad & \left\{ \begin{aligned} \frac{dM}{dx} &= \frac{(2 + (\gamma - 1)M^2)M}{2\sqrt{M^2 - 1}} \frac{d\theta}{dx} - \frac{M_p}{h} \frac{2 + (\gamma - 1)M^2}{2[(M^2 - 1) \cos \theta - \sqrt{M^2 - 1} \sin \theta]} \end{aligned} \right.
 \end{aligned} \tag{4}$$

where  $M = (u^2 + v^2)^{1/2}/a$  is the local Mach number,  $\theta = \arctg(v/u)$  is the angle between the velocity and the axial direction,  $\gamma$  is the isentropic constant of the gas and  $M_p = w_p/a_1$  is a velocity coefficient which takes into account the parietal injection (strictly speaking,  $M_p$  must be defined with respect to the local sound velocity, but within the framework of the simplifying assumptions used here, the velocity of sound  $a_1$  at the cascade input can be replaced by  $a$  and leads to a constant parameter).

#### II.4. Boundary Conditions

##### II.4.1. At the cascade input.

We only consider operation in the supersonic range [3], and the periodicity of the flow, i.e., the condition of "unique incidence" [4], determines the conditions at the cascade input. In the examples presented below the top phase of the profile of the cascade consists of a rectilinear part in the vicinity of the top phase and in such a way that the flow is uniform in the input plane of the cascade.

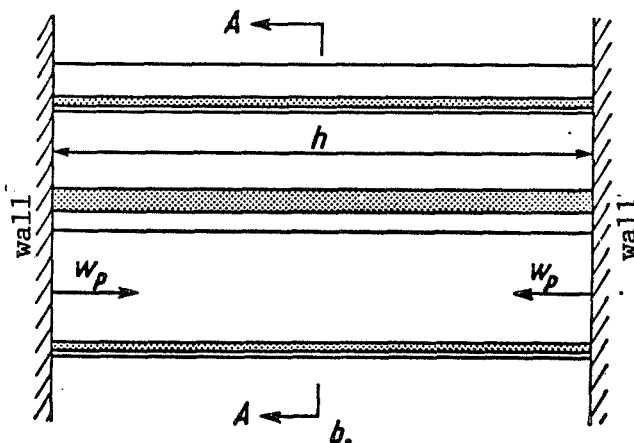
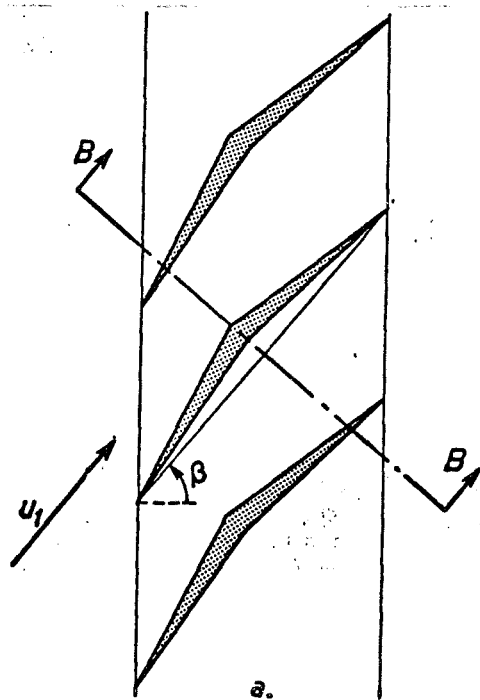


Figure 1. Longitudinal and transverse cross sections through a supersonic cascade.

- a) Longitudinal cut - AA.
- b) Transverse cut - BB.

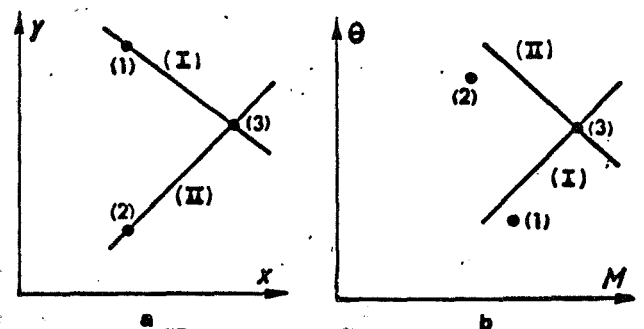


Figure 2. Determination of the running point.

- a) Physical plane
- b) Hodograph plane

#### II.4.2. Along the profile.

Since the profile geometry is known, the condition that the velocity is parallel to the tangent to the wall defines the angle  $\theta$  between the velocity and the normal and the front of the cascade.

#### II.4.3. Through a shock wave.

Since the shock wave thickness is infinitely small, the correspondence relationships established in the two-dimensional theory [5], for shock waves remain in effect.

$$\begin{cases} \operatorname{tg} \sigma = \frac{2}{\gamma + 1} \operatorname{tg} (\sigma - \psi) \left[ \frac{1}{M_2^2 \sin^2 (\sigma - \psi)} + \frac{\gamma - 1}{2} \right] \\ \frac{1}{\operatorname{tg} \psi} = \left[ \frac{\gamma + 1}{2} \frac{M_1^2}{M_1^2 \sin^2 \sigma - 1} - 1 \right] \operatorname{tg} \sigma \end{cases} \quad (5)$$

where  $M_1$  and  $M_2$  are the Mach numbers ahead and downstream of the shock wave.  $\sigma$  is the angle between the shock and the incident flow,  $\psi$  is the angle of flow deflection through the shock. In the remainder of the calculations we will only be interested in the solution for which the flow remains supersonic after the shock wave (weak shock) which can be translated into the condition

$$1 < M_2 < M_1.$$

### III. Method of Integration

#### III.1 Running Point

The numerical integration methods for supersonic flow equations [6] can be generalized in the case considered here. Thus, in order to determine the coordinates of the point (3) located at the intersection of the characteristics (I) emanating from (1), and (II) emanating from (2) (Figure 2), the equations for (4) can be written in the form of finite increments. The following relationships are obtained in the physical plane:

$$\begin{cases} x_3 = \frac{y_1 - \delta'_{1,3} x_1 - (y_2 - \delta''_{2,3} x_2)}{\delta''_{2,3} - \delta'_{1,3}} \\ y_3 = \frac{\delta''_{2,3} (y_1 - \delta'_{1,3} x_1) - \delta'_{1,3} (y_2 - \delta''_{2,3} x_2)}{\delta''_{2,3} - \delta'_{1,3}} \end{cases} \quad (6)$$

In the hodograph plane these relationships are:

$$M_3 = \frac{\xi_{2,3} M_1 + \xi_{1,3} M_2 + \xi_{1,3} \xi_{2,3} (\theta_1 - \theta_2) - A_1 \left\{ \frac{\xi_{2,3} \alpha_{1,3}}{\beta'_{1,3}} (x_3 - x_1) + \frac{\xi_{1,3} \alpha_{2,3}}{\beta''_{2,3}} (x_3 - x_2) \right\}}{\xi_{1,3} + \xi_{2,3}}$$

$$\theta_3 = \frac{M_1 - M_2 + \xi_{1,3} \theta_1 + \xi_{2,3} \theta_2 + A_1 \left\{ \frac{\alpha_{2,3} (x_3 - x_2)}{\beta''_{2,3}} - \frac{\alpha_{1,3}}{\beta'_{1,3}} (x_3 - x_1) \right\}}{\xi_{1,3} + \xi_{2,3}}$$

The correspondence between the parameters  $\alpha$ ,  $\beta$ ,  $\delta$ ,  $\xi$ , and  $A_1$  and the initial and final values of the parameters  $M$  and  $\theta$  is given in table I:

TABLE I

$$\begin{aligned}
\delta_{n,q}^I &= \frac{M_{n,q}^2 \cos \theta_{n,q} \sin \theta_{n,q} - \sqrt{M_{n,q}^2 - 1}}{M_{n,q}^2 \cos^2 \theta_{n,q} - 1} \\
\delta_{n,q}^{II} &= \frac{M_{n,q}^2 \cos \theta_{n,q} \sin \theta_{n,q} + \sqrt{M_{n,q}^2 - 1}}{M_{n,q}^2 \cos^2 \theta_{n,q} - 1} \\
\alpha_{n,q} &= \frac{2 + (\gamma - 1) M_{n,q}^2}{2 \sqrt{M_{n,q}^2 - 1}} \\
\xi_{n,q} &= \alpha_{n,q} M_{n,q} \\
\beta_{n,q}^I &= \cos \theta_{n,q} \sqrt{M_{n,q}^2 - 1} + \sin \theta_{n,q} \\
\beta_{n,q}^{II} &= \cos \theta_{n,q} \sqrt{M_{n,q}^2 - 1} - \sin \theta_{n,q} \\
A_1 &= \frac{M_p}{h} \\
M_{n,q} &= \frac{M_n + M_q}{2} \\
\theta_{n,q} &= \frac{\theta_n + \theta_q}{2}
\end{aligned}$$

An iteration calculation is necessary in order to determine the coordinates and the velocity components at (3) from the points (1) (2). This iteration calculation is terminated when an accuracy criterion is satisfied.

### III.2 Point of Intersection with a Solid Wall.

As an example, let us present the equations which govern the encounter of a characteristic (I) with a wall having an angle  $\omega$  with the axis  $Ox$ . The point (3) corresponding to intersection of the characteristic

(I) emanating from point (1) (Figure 3) with the wall can be determined by means of the equation:

$$\begin{cases}
x_3 = \frac{y_2 - x_2 \operatorname{tg} \omega - (y_1 - \delta_{1,3}' x_1)}{\delta_{1,3}' - \operatorname{tg} \omega} \\
y_3 = \frac{\delta_{1,3}' (y_2 - x_2 \operatorname{tg} \omega) - (y_1 - \delta_{1,3}' x_1) \operatorname{tg} \omega}{\delta_{1,3}' - \operatorname{tg} \omega} \\
\theta_3 = \omega \\
M_3 = M_1 - \xi_{1,3} (\theta_3 - \theta_1) - A_1 \frac{\alpha_{1,3}}{\beta_{1,3}'} (x_3 - x_1)
\end{cases} \quad (8)$$

and the same kind of iterations as those used for the determination of the running point.

### III.3. Point Located in the Center of an Expansion Bundle (Prandtl-Meyer Expansion).

When the wall has a break  $\delta\omega$  an expansion fan emanates from this point,



which from a mathematical point of view behaves like a multiple point. An infinite number of characteristics of one of the families emanates from this point. The numerical method utilized separates this bundle into  $k$  discrete waves which each correspond to a deviation

$$\delta\theta = \frac{\delta\omega}{k} \quad (9)$$

of the flow. These characteristics are given by the equations:

$$M_j - M_i = \mp \xi_{i,j} \frac{\delta\omega}{k} \quad (10)$$

depending on whether they originate along the lower or upper wall. The indices  $i$  and  $j$  have the definition indicated in Figure 4.

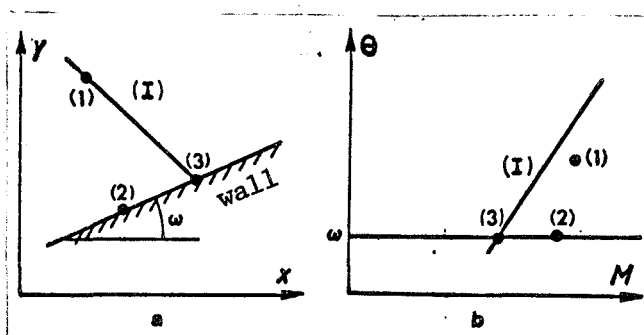


Figure 3. Intersection of a characteristic with a wall.

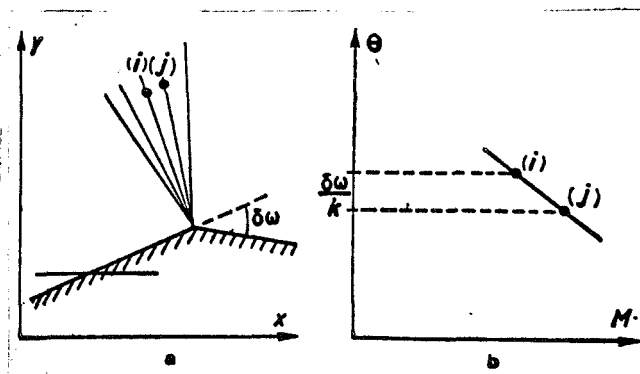


Figure 4. Point located in an expansion bundle.

- a) Physical plane
- b) hodograph plane

Just as in any supersonic motion, shock waves can appear in the flow. A different calculation can be carried out depending on whether we are dealing with a point at which the shock originates or running point along the shock.

#### IV.1. Point of Origination of a Shock Wave

Here we will only consider the case where due to the sharp variation in the slope of one wall of the assembly, so as to reduce the cross section of the channel, a shock wave appears in the fluid (Figure 5). The method we will use is the one developed by P. Diringer and P. Laval.

Equations (6) and (7) are used to determine the  $K^-$  conditions for  $K$  at the angular point of the wall. The correspondence Equations (5) without a shock wave are used to determine the conditions  $K^+$  downstream of a shock for a deflection  $\psi$ .

#### IV.2. Running Point along the Shock Wave

The calculation of a running point along a shock wave requires interpolations as well as the iterations mentioned above. This is because the shock wave does not pass through the nodes of the grid of characteristics. The principle of calculations is adapted from [6]. This entails determining the point along the  $n^{\text{th}}$  characteristics of family II from the variables given along the  $(n-1)^{\text{th}}$  characteristics of the same family (Figure 6).

The calculation is straightforward up to the point  $J_n$ . First, the point is on the same characteristic  $II_n$  located at the intersection point of the family I characteristic emanating from point  $K_{n-1}^-$ . It is located at the upstream edge of the shock wave at its intersection point with  $II_{n-1}$ . The conditions

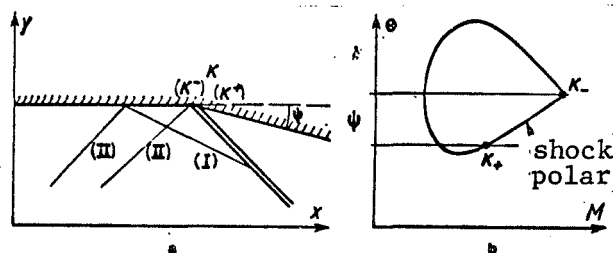


Figure 5. Conditions at the beginning point of a shock wave.

- a) Physical plane
- b) Hodograph plane

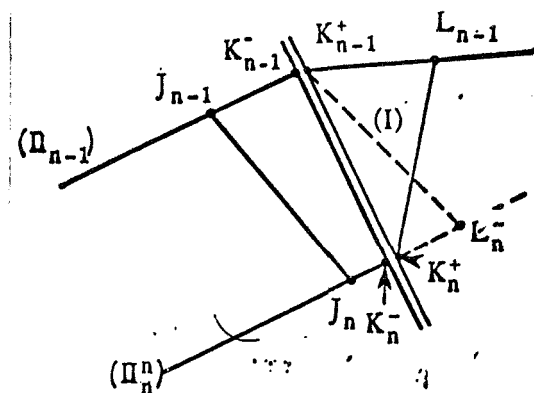


Figure 6. Determination of the present point  $K (K_n^-, K_n^+)$  of the shock wave at the  $J_n$  intersection with the characteristic  $II_n$ .

at  $K_n^-$  are obtained by linear interpolation between  $J_n$  and  $L_{n-1}$ . The conditions along the upstream shock wave front  $K_n^+$  are derived in the same way from the characteristics emanating from an appropriate point  $L_{n-1}$  of the downstream part of the  $II_{n-1}$  characteristic. The point is correctly chosen if the conditions  $K_n^-$  and  $K_n^+$  correspond to the relationships (5).

The calculation is slightly complicated if the point  $L_{n-1}$  can not be determined along the characteristic  $II_{n-1}$ , due the fact that the wall is too close. It is then necessary to introduce an interpolation characteristic  $II_{n-1}^*$ . Its point of origination along the downstream edge of the shock wave is chosen so that after reflection from the wall at  $L_{n-1}$  a family I characteristic is produced which passes through  $K_n^+$  (Figure 7). This calculation is applied in the vicinity of the point of origination of the shock wave.

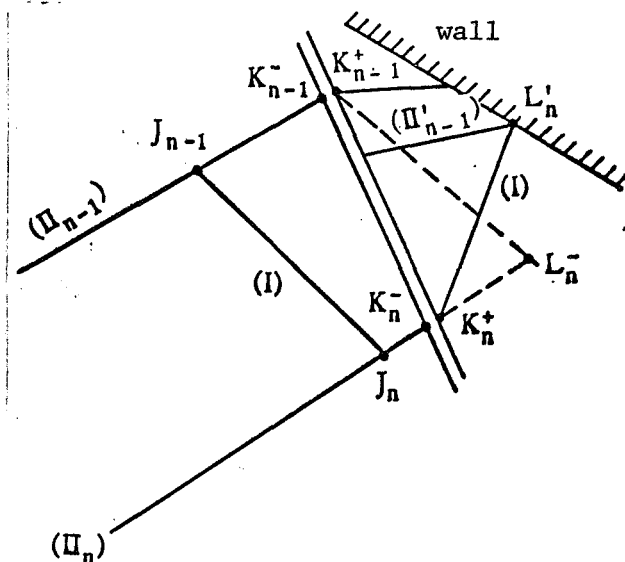


Figure 7. Determination of the present point  $K_n(K_n^-, K_n^+)$  of the shock wave in the vicinity of its initial point.

#### V. Cascade with Plane Plates

The most simple application of the preceding calculations is the application to a cascade with plane plates. We studied the one-dimensional flow with a transverse velocity component as an example in order to protect the program. Physically, such a flow corresponds to the case of a cascade having normal flat plates along the front of the cascade. There is also a lateral thickening of the boundary layer (Figure 8a). A two-dimensional representation consists of a uniform flow in which infinitesimally thin flat plates are inserted without incidence (Figure 8b). The thickening of the boundary layer along the lateral walls is represented by a constant normal velocity in the plane of the cascade.

The equations of motion (3) can be reduced to the following if there is no vertical component  $v$ :

$$\begin{cases} (a^2 - u^2) \frac{du}{dx} - a^2 \frac{w_p}{h} = 0 \\ a^2 = a_0^2 - \frac{\gamma - 1}{2} u^2 \end{cases} \quad (11)$$

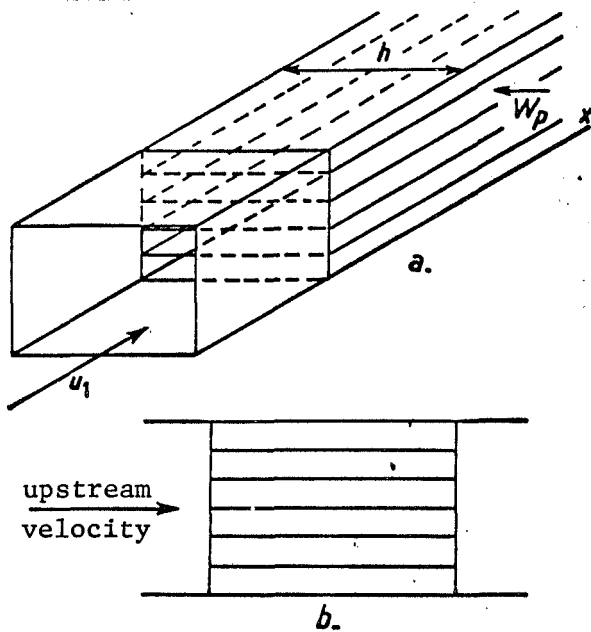


Figure 8a. Diagram of a cascade with plane plates parallel to the wind.

Figure 8b. Cross section of the cascade with plane plates by plane normal to the cascade.

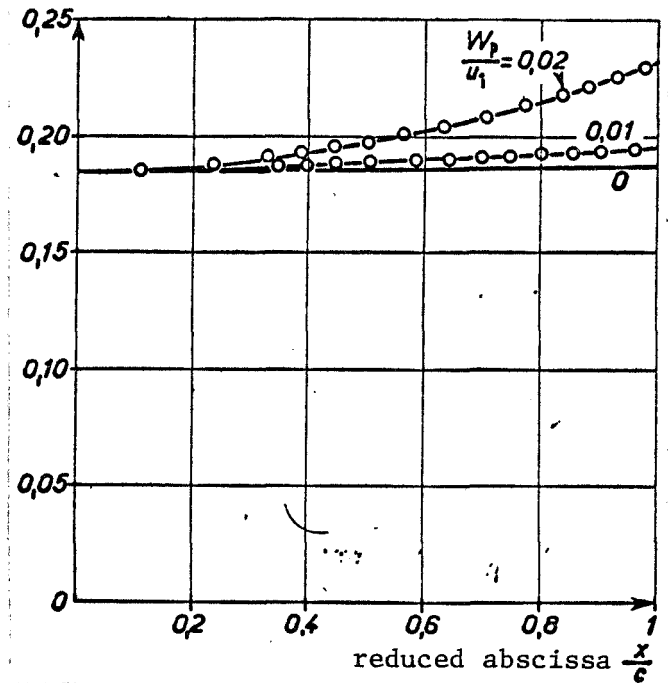


Figure 9. Comparison of the pressure distribution along the upper and lower surfaces of the plates at the pressure calculated by means of the one-dimensional method.

The integral of this equation can be written as:

$$\frac{w_p x}{h} = \frac{\gamma + 1}{\gamma - 1} u - \frac{a_0}{\gamma - 1} \sqrt{\frac{2}{\gamma - 1}} \log \frac{a_0 \sqrt{\frac{2}{\gamma - 1}} + u}{a_0 \sqrt{\frac{2}{\gamma - 1}} - u} + \text{Const.} \quad (12)$$

The constant is determined by the condition  $u = u_1$  for  $x = 0$ .

The pressure distribution derived from this one-dimensional calculation was compared in Figure 9 to that obtained by means of a two-dimensional method for a Mach number of  $M_1 = 1.8$  at the inlet of the cascade. The following values of the parameter which determine the magnitude of the transverse velocity were used

$$\frac{w_p}{u_1} = 0; 0.01 \text{ and } 0.02$$

(The index 1 refers to the inlet of the cascade). It can be seen in Figure 9 that the effect of transverse wind is far from negligible as far as the pressure distribution is concerned. However, in the case considered here, no blade lift occurs.

#### VI. Cascade with a Double-Triangle Profile

In order to compare the predictions given by the calculations to experimental results, the flow in a cascade having a double-triangle profile (Figure 1) was analyzed. Complete experimental results are available for this cascade [7]. This makes it possible to make a connection between theory and experiment. The construction data and experimental data of the cascade studied are collected in Table II.

TABLE II

Study of supersonic, double-triangle blades.

Chord	60 mm
Step	30 mm
Leading edge angle of attack	6°
Upper angle of twist	18°
Set angle	60°
Upstream Mach number	1.75

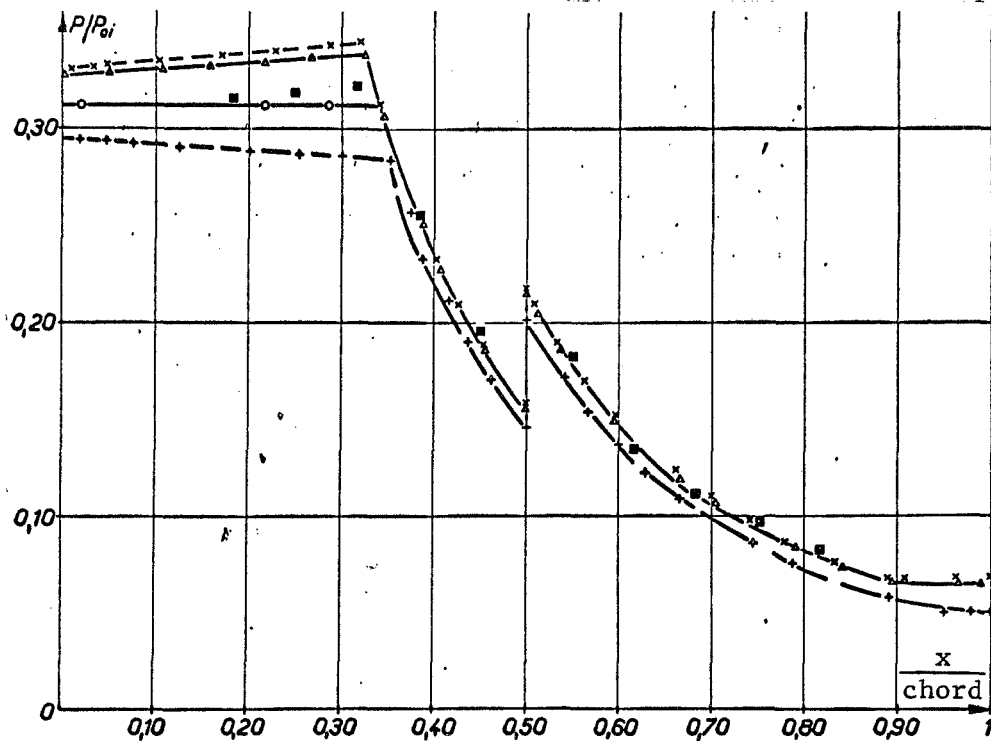


Figure 10a. Distribution of the pressure on top; double-triangle cascade.

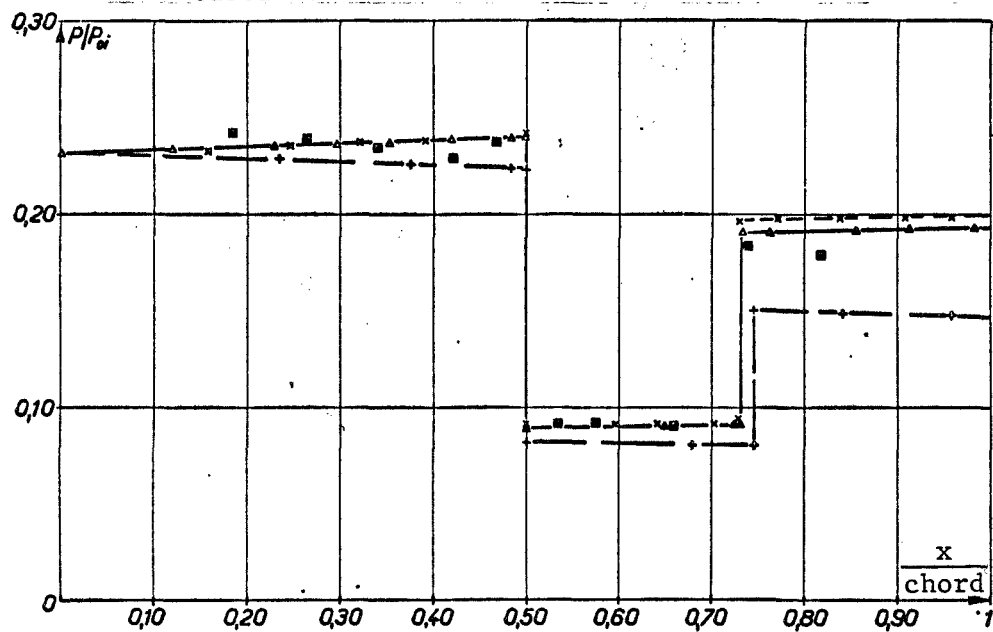


Figure 10b. Distribution of the pressure below; double-triangular compressor.

Figure 10 shows the pressure variations of the upper and lower surfaces for various magnitudes of the transverse wind:

$$\frac{w_p}{u_1} = -0,014; 0; 0,010; 0,014; 0,020$$

as well as the experimental points, recorded at mid-span. The substantial influence of the lateral wind on the pressure distribution along the blades is quite noticable. Since the experimental points lie essentially along the curve corresponding to  $w_p = 0$ , it can be concluded that the mid-span cross section of the blade essentially behaves as though it were placed in a two-dimensional flow.

#### VII. Conclusion

The method of characteristics developed for the study of two-dimensional supersonic flows can be applied to the case of a motion having in addition a transverse velocity component, as is encountered in supersonic compressors with a strong convergence stream. In their particular case of tests of supersonic cascades, the calculation carried out made it possible to show that the measurements carried out at mid-span of the blades correspond well with plane flow. This means that the measured cross section is not influenced by the interaction of parietal boundary layers.



## References

1. Shaalan, R. A. and J. H. Horlock. The Effect of Change in Axial Velocity on the Potential Flow in Cascades. ARC (A.-M.) Vol.3547, Sept. 1966.
2. Mani, A. and A. J. Acosta. Quasi-Two-Dimensional Flows Through a Cascade ASME Journal of Engng for Power, April, 1968.
3. Fabri, J. The Different Operating Regions of Supersonic Compressors. Note Technique O.N.E.R.A. No. 145, 1969.
4. Chauvin, J, F. Breugelmans, and A. Janigro. Supersonic Compressors. Supersonic Turbo-Jet Propulsion Systems and Components. AGARDograph Vol. 120, 1970.
5. Carriere, P. Methods for the Study of Supersonic Flows. Publ. Sc. and Tech du Minstere de l'Air Paris. No. 339a, 1964.
6. Diringer, P and P. Laval. Calculation of Steady Supersonic Flows Around Profiles or Bodies of Revolution, with or without Incidence by the Method of Characteristics. Note Technique O.N.E.R.A. No. 126, 1968.
7. Fabri, J. J. Paulon, and G. Janssens. Use of Supersonic Cascades Made of Blades of Simple Geometric Shapes for Cascade Wind Tunnel Performance Evaluation. ASME Bruxelles -- Gas Turbine Conference, paper 70-GT-110. 1970

Translated for National Aeronautics and Space Administration under Contract No. NASw-2035, by SCITRAN, P. O. Box 5456, Santa Barbara, California, 93103.